Smart Structures and Systems, *Vol. 34*, *No. 4* (*2024*) *261-270*
https://doi.org/10.12989/sss.2024.34.4.261

Dynamic control of nonlinear structural systems by smart linear quadratic regulator algorithm

Yahui Meng [1], ZY Chen[***1], Ruei-Yuan Wang[**1] and Timothy Chen[*2]

[1] *School of Science*, *Guangdong University of Petrochemical Technology*, *Maoming 525000*, *Peoples R. China*
[2] *Engineering and Applied Science*, *California Institute of Technology*, *Pasadena*, *CA 91125*, *USA*

(*Received March 7*, *2024*, *Revised September 26*, *2024*, *Accepted November 10*, *2024*)

Abstract. This article aims investigating the efficiency of the smart advanced control algorithm applied to the structural dynamic analysis with leaner quadratic regulator (LQR). We chose the linear-quadratic regulator algorithm to drive the system into the desired state, where the optimal control strategy considers minimization task of the cost-to-go functional with respect to the state error and control effort. Our main contribution in this paper is the development of a fast and scalable feasible solution for building nonlinear structural analysis. Thus, we seek to accommodate a time varying fuzzy model by LQR algorithm with the proposed smart modelling for design and analysis in systems. We provide a detailed theoretical formulation and its numerical implementation in a variational format form. Several illustrative numerical examples are provided to confirm an excellent performance of the proposed methodology. The objectives of this paper are access to adequate, safe and affordable housing and basic services, promotion of inclusive and sustainable urbanization and participation, implementation of sustainable and disaster-resilient buildings, sustainable planning and management of human settlement. Therefore, the goal is believed to be achieved in the near future through the continuous development of AI and control theory for a better life from the environment and built systems.

Keywords: artificial intelligence tools; fuzzy models; linear-quadratic regulator; nonlinear structural dynamics system; optimal control; smart structure

1. Introduction

With a quest for increasing renewable energy share, the research Schematic of the path planning problem (see Fig. 1) is exploring technological innovation towards multibody systems in engineering structural practical applications. Fig. 1(a) represents the continuous state-space: The autonomous agent must travel from x0 to xf in a domain under the influence of a stochastic dynamic flow field v(x, t; wv) and a stochastic dynamic scalar field g(x, t; wg) (e.g., solar radiation). The agent takes an action a = π (x, t) according to an optimal deterministic policy x and is simultaneously advected by an instantaneous velocity v. Such improvement requires corresponding contributions in nonlinear dynamics and, more precisely, the numerical models of large engineering will provide improved safety under extreme climate conditions. Also, in order to control stability and avoid damage (Toma and Chen 2024, Ahmad and Shokouhian 2024), we need to provide the corresponding algorithms for control of the vibrations of the geometrically exact beam that is used as the basic ingredient in constructing the numerical model of flexible wind-turbine blades. In order to ensure the desired response of the structure and suppress its vibrations, many papers and books are focused on searching for the most appropriate control algorithm. The proportional-integral-derivative (PID) controllers have been used for many years for linear problems, due to their simplicity, efficiency and reliability, PID controllers and their different modifications are still the most popular to use for control processes of flexible systems. Special attention is focused on optimization of PID controller parameters. To design an optimal analogue and discrete PID controller, an analogue and discrete time linear quadratic regulator (LQR) as suggested in (Zhou 2023, Ariyanto *et al*. 2023, Zhu 2023, Zhou *et al*. 2023, 2024, Zheng *et al*. 2022, 2023). Optimal tuning of PI/PID controller for time-delay processes using LQR is further proposed in (Zhang *et al*. 2023, 2024, Yin *et al*. 2024, Wu *et al*. 2022, Wang *et al*. 2023a). Many studies have investigated the control problems of the flexible system mechanics. In addition to other analyses, (Wang *et al*. 2024c, d, Tian *et al*. 2024a, Song *et al*. 2024, Shu *et al*. 2025, Mohammadzadeh *et al*. 2024) gave a critical review of control algorithms applied to rotating composite beams and blades. The position control of a flexible four bar mechanism has been provided by PID controller while proportional controller has been used to suppress vibration in (Miaofen *et al*. 2023, Liu *et al*. 2023, Shi *et al*. 2023b, Tan *et al*. 2023, Li *et al*. 2021, 2024a, b). Optimal control

*Corresponding author, Mr.,
E-mail: t13929751005@gmail.com
**Co-corresponding author, Mr.,
E-mail: rueiyuan@gmail.com
***Co-corresponding author, Mr.,
E-mail: president@gdupt.edu.cn

ISSN: 1738-1584 (Print), 1738-1991 (Online)

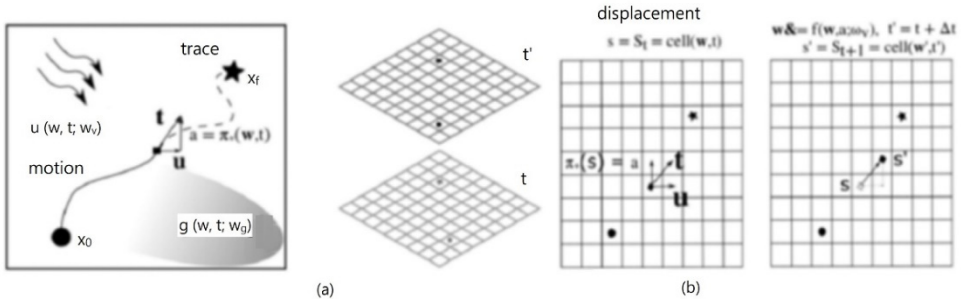

Fig. 1 Schematic of the path planning problem

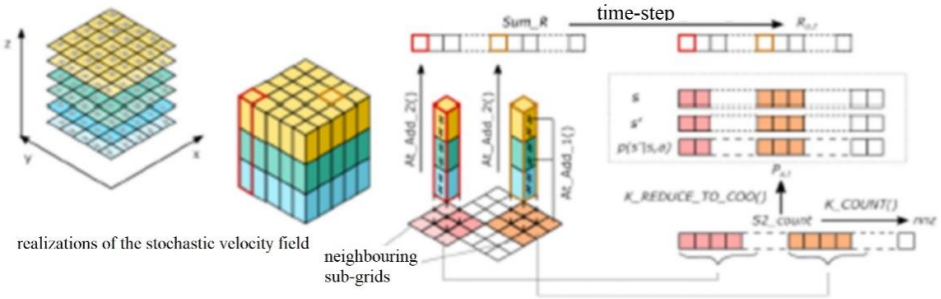

Fig. 2 Methodology for building the MDP model using a GPU

algorithms, based on linear quadratic regulator (LQR), are very popular due of their robustness and has been used to improve overall performances of flexible structures (Kai and Yin 2022, Hirao *et al*. 2023, Guo *et al*. 2023, Du *et al*. 2024) for Stewart platform with flexible legs (Shi *et al*. 2023b), flexible beam linkage (Chen *et al*. 2022a, Chai *et al*. 2024), flexible riser (Song *et al*. 2021), and Timoshenko beam (Cao *et al*. 2024).

Active vibration control of a piezoelectric beam was investigated in (Tan *et al*. 2023), where several different popular control strategies were applied and compared: LQR and Linear Quadratic Gaussian controller (LQG) in (Tian *et al*. 2024b) and mixed LQR regulator (Wang *et al*. 2023b). More works on control theory can be referenced in the books of (Xu *et al*. 2022). The main novelty of this work lies in the selection of the most suitable strategy from among numerous control algorithms to control the vibrations of a geometrically accurate Reissner beam. In this paper, we still use the optimal control based on the LQR algorithm, but consider the tangential stiffness change caused by the nonlinear form of the Kalman gain based on the Riccati solution.

We briefly introduce a geometrically accurate beam model for representing large motions of flexible blades in a nonlinear dynamic framework. In Section 3, we present the corresponding development of optimal nonlinear control for models with state feedback loops, and then present the results of numerical simulations in Section 4.

2. Preliminary of smart control

We consider the analysis of concrete structure models, if the vibration damping ratio parameter of the first period of the concrete structure is set to 2%, and the remaining periods are all below 10%, see Fig. 2, in which methodology for building the MDP model using a GPU by 3-D grid showing various realizations of the stochastic velocity field at a given time-step by 3-D grid of CUDA threads. The expression of the vibration damping ratio in the first period is shown in Eqs. (1)-(2).

$$\boldsymbol{\phi} = \boldsymbol{\varphi} + x_2\mathbf{t}_2; \quad \boldsymbol{\varphi} = (x+u)\mathbf{e}_1 + (y-v)\mathbf{e}_2 \tag{1}$$

$$\xi_i = min\left\{\frac{\omega_i}{50\omega_1}, 0.1\right\} \qquad (i = 2, L, n) \tag{2}$$

At this moment, the damping matrix is expressed as shown in Eq. (3).

$$C = M\Phi\Lambda[2\xi_1\omega_1, 2\xi_2\omega_2, L, 2\xi_n\omega_n]\Phi^{-1} \tag{3}$$

In Eq. (3), Φ denotes the formation matrix; ξ_i is the damping ratio of the i period; ω_n indicates the natural frequency of the i period. The concrete structure equation is shown in Eq. (4).

$$\dot{Z}(t) = AZ(t) + BU(t) + DF(t) \tag{4}$$

In Eq. (4), A, B, and D are expressed under

$$M^{-1}K = \Phi \tag{5}$$

which refers to the formation matrix; $0_{n\times n}$, $0_{n\times p}$, $0_{n\times q}$ express the $n\times n$, $n\times p$, $n\times q$ dimensional zero matrix; B_s stands for the actuator displacement matrix; $I_{n\times n}$ expresses the identity matrix. The fuzzy domain set is defined as U, and its expression is shown in Eq. (6).

$$U = \{u_1, u_2, \ldots, u_n\} \tag{6}$$

In Eq. (6), $u_1, u_2, \ldots, u_n$ indicate domain set. The membership function is determined by fuzzy statistics, and the variable set of cloud top boundary belonging to the set U is defined as A^*. The element u_i of the sub test subset in n belongs to A^*, which is expressed as $n_{A^\bullet}$. A stable $n_{A^\bullet}/n$ ratio can be obtained through multiple experiments, and then u_i belongs to the fuzzy set A membership, which is expressed in Eq. (7).

$$u_A(u_i) = \lim_{n\to\infty} \frac{n_{A^\bullet}}{n} \tag{7}$$

In Eq. (7), A denotes the borderless and $A^\bullet$ consistent fuzzy set; n means the amount of tests; u_i represents the amount of $u_i \in A^\bullet$ in the n test.

Due to the fact that different inference results in fuzzy reasoning correspond to different degrees of membership, the maximum one of these degrees of membership is used as the output, as shown in Eq. (8).

$$u_0 = \max u_A(u) \quad u \in U \tag{8}$$

In the process of fuzzy reasoning, there are multiple outputs corresponding to the max membership degree, and the mean of all corresponding values is selected as the final output value, as expressed in Eq. (9).

$$u_0 = \frac{1}{J}\sum_{j=1}^{J} u_j \tag{9}$$

Among them, u_j and J are expressed as shown in Eq. (10).

$$\begin{cases} u_j = \max\limits_{u\in U}\left(u_A(u)\right) \\ J = |\{u\}| \end{cases} \tag{10}$$

According to the constitutive equation of magnetic current in the stable shear field, this state can be described, as shown in Eq. (11).

$$\tau = \tau_y sgn(\dot{\gamma}) + \eta\dot{\gamma} \tag{11}$$

In Eq. (11), τ_y denotes the yield of the magnetorheological fluid; τ means the total shear stress of the magnetorheological fluid; $\dot{\gamma}$ refers to the parameters of the magnetized fluid. When the particles do not meet magnetic saturation, the shear yield under the theory of magnetorheological fluid is expressed in Eq. (12).

$$\tau_y = \sqrt{6}\phi\mu_0 M_s^{1/2} H_0^{2/3}) \tag{12}$$

In Eq. (12), M_s stands for the magnetization intensity of the saturated particle state; ϕ means the particle content of the magnetorheological fluid; μ_0 refers to the true permeability; H_0 represents the applied magnetic field intensity. A valve type damper and shear damping force, as expressed in Eq. (13).

$$\begin{aligned} F = &\left[\frac{3\pi\eta L(D^2-d^2)}{4Dh^3} + \frac{L\pi D\eta}{h}\right]v \\ &+\left[\frac{3\pi L(D^2-d^2)}{h} + L\pi D\right]\tau_y sign(v) \end{aligned} \tag{13}$$

In Eq. (13), η stands for the apparent density of the magnetorheological fluid; $sign(v)$ indicates the piston motion control function; h means the particle gap of the magnetorheological fluid; D means the piston diameter; d refers to the internal diameter of the piston; L stands for the effective length of the piston. According to Eqs. (12) and (13), the shear type MRFD model can be simplified, as shown in Eq. (14).

$$\begin{aligned} F_{sv} = &\frac{3\eta L[\pi(D^2-d^2)]^2\tau_y}{4Dh^3}v \\ &+\frac{3L\pi(D^2-d^2)}{4h}\tau_y sng(v) \end{aligned} \tag{14}$$

According to Eq. (14), the model is composed of two terms. The first term mainly considers fluid power viscosity, which is a fixed value.

$$\beta_v = \frac{bh^2\tau_y}{4\eta Q} = \frac{Dh^2\tau_y}{\eta(D^2-d^2)v} \tag{15}$$

In Eq. (15), v denotes the piston speed and b expresses the Coulomb damping characteristic parameter. In the research, fuzzy DC strategy is mainly used and compared with traditional linear quadratic regulator (LQR) control strategy to achieve good performance indicators of the original system at low cost.

$$\begin{aligned} K &= \frac{1}{2}\int_L \int_A \rho\phi^T\cdot\phi dAds \\ &= \frac{1}{2}\int_L \left(A_\rho\dot{\varphi}^T\cdot\dot{\varphi} + J_\rho\psi^2\right)ds \end{aligned} \tag{16}$$

with energy given in Eqs. (10) and (16)

$$H(\varphi,\psi;\dot{\varphi},\dot{\psi}) = K(\dot{\varphi},\dot{\psi}) + \Pi(\varphi,\psi) \tag{17}$$

$$\begin{aligned} &G(\varphi,\psi;\delta\varphi,\delta\psi) \coloneqq \int_L \left(\delta\varphi^T\cdot A_\rho\ddot{\varphi} + \delta\psi\cdot J_\rho\ddot{\psi}\right)ds \\ &+\int_L \left((\delta\varphi' - \delta\psi\mathbf{W}\varphi')^T\cdot\mathbf{n} + \delta\psi'\mathbf{e}_3^T\cdot\mathbf{m}\right)ds - G^{ext} \\ &= 0 \end{aligned} \tag{18}$$

where the static term corresponds to the one already stated in Eq. (11).

3. Optimal nonlinear design with state feedback loop

In this section, we consider the development of modern control algorithms (see Fig. 3). Such a process involves dynamic optimization with respect to an operating cost

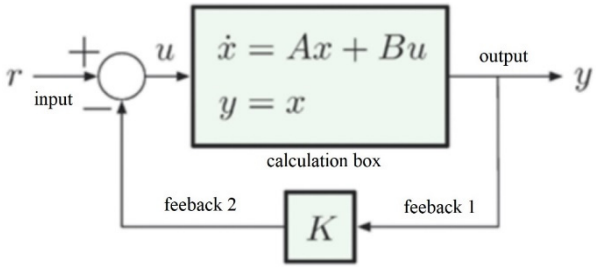

Fig. 3 Control process

function (also called an exponential performance or revenue function) and imposed boundary conditions, with the goal of achieving optimal operation of the system. The key elements of the optimal control problem can be expressed as follows: i) Mathematical model, as shown in Eq. (1). (18), represented by a set of nonlinear differential equations, ii) the specification of the operating cost function from which we derive the optimal control law by finding extrema, iii) the imposition of boundary conditions on the state and/or control.

We note that the optimization procedure for this type of problem is standard, but the complexity may vary depending on the type of control we wish to achieve. Furthermore, dynamic optimization tasks involve time-varying conditions and system variables, which are more challenging than controlling the system under steady-state conditions (see Xu and Li 2024). We further trace the necessary steps in nonlinear control design to formulate an optimal control law for a finite-time linear quadratic regulator.

3.1 State-space equations

To simplify the analysis, it is common to reconvert the motion references into the so-called state space form, resulting in a set of first-order differential equations describing the system response in dynamics. We first modify the linearized form of the dynamic equilibrium proposed in Eq. (18), select the first state variable vector as $\boldsymbol{x}_1(t) = (\boldsymbol{\varphi}(t), \psi(t))T$

$$\mathbf{M}\ddot{\mathbf{x}}_1(t) + \mathbf{K}(t)\mathbf{x}_1(t) = \mathbf{f}^{ext}(t) + \mathbf{u}(t) \tag{19}$$

By further selecting another state space vector $\mathbf{x}_2(t) = \dot{\mathbf{x}}_1(t) = \big(\dot{\boldsymbol{\varphi}}(t), \dot{\psi}(t)\big)T$, we can obtain the state-space representation

$$\begin{cases} \dot{\mathbf{x}}_1(t) = \mathbf{x}_2(t) \\ \dot{\mathbf{x}}_2(t) = \mathbf{M}^{-1}\big(\mathbf{K}(t)\mathbf{x}_1(t) + \mathbf{u}(t)\big) \\ \mathbf{x}_1(0) = \mathbf{x}_1^0 \\ \mathbf{x}_2(0) = \mathbf{x}_2^0 \end{cases} \tag{20}$$

where $\mathbf{x}_1(0)$and $\mathbf{x}_2(0)$ are the initial conditions. With this state space representation, it is given in Eq. (20), we reduce the order of the differential equation from second order to first order. Therefore, we can apply standard numerical solution procedures that are more stable and accurate. On the other side, the number of differential equations has doubled, from n to $2n$, which implies a higher computational cost. However, this increase in computational cost is often outweighed by the benefits that the state-space form offers in terms of numerical stability, analysis and control design.

A standard state-space representation can be given in matrix form, by introducing $\dot{\mathbf{x}}(t) = \big(\dot{\mathbf{x}}_1(t), \dot{\mathbf{x}}_2(t)\big)T$ in Eq. (20) as follows

$$\underbrace{\begin{Bmatrix} \dot{\mathbf{x}}_1(t) \\ \dot{\mathbf{x}}_2(t) \end{Bmatrix}}_{\dot{\mathbf{x}}(t)} = \underbrace{\begin{bmatrix} 0 & \mathbf{I} \\ -\mathbf{M}^{-1}\mathbf{K}(t) & 0 \end{bmatrix}}\underbrace{\begin{Bmatrix} \mathbf{x}_1(t) \\ \mathbf{x}_2(t) \end{Bmatrix}}_{\mathbf{x}(t)} + \underbrace{\begin{Bmatrix} \mathbf{0} \\ \mathbf{M}^{-1} \end{Bmatrix}}_{\mathbf{B}}\boldsymbol{u}(t) \tag{21}$$

where $\mathbf{A} \in \mathbb{R}mxm$ and $\mathbf{B} \in \mathbb{R}mxm$ are state (or system) and input matrices. The expression in Eq. (21) can be rewritten in more compact form as

$$\dot{\mathbf{x}}(t) = \underbrace{\mathbf{A}(t)\mathbf{x}(t) + \mathbf{B}\mathbf{u}(t)}_{\mathbf{f}(\mathbf{x}(t),\boldsymbol{u}(t),t)} \equiv \mathbf{f}(\mathbf{x}(t), \boldsymbol{u}(t), t) \tag{22}$$

where $\boldsymbol{f}(\boldsymbol{x}(t), \boldsymbol{u}(t), t)$ is a state function. Since we consider time-varying systems, we note that only the state matrix $\boldsymbol{A}(t)$ changes in time, while the input matrix $\boldsymbol{B}$ remains constant. However, the following development should hold for both cases.

3.2 Preliminary for LQR algorithm

The basic concept of optimal control involves various forms of cost functions that can be formulated based on minimization objectives, including factors such as time control, energy control, terminal error, etc. Such a cost operating function J represents a quantitative measure of how well a controlled dynamic system performs over a specific period of time, so the general form of this function can be given

$$J = \Phi\big(\mathbf{x}(t_f), t_f\big) + \int_{t_0}^{t_f} L(\mathbf{x}(t), \boldsymbol{u}(t), t)dt \tag{23}$$

where the terms $\Phi(\cdot)$ and $\int L(\cdot)dt$ are given as a quadratic form representing terminal constraint at the final time and the sum of the cost rates, respectively. The integral function $L(\cdot)$ is also referred to as Lagrangian. Furthermore, we exploit the additive interval property of integrals to state the incremental change in the cost-to-go function for the time interval $[t, t+\Delta t]$

$$\begin{aligned} &J(\mathbf{x}(t), t) \\ &= \int_t^{t+\Delta t} L(\mathbf{x}(t), \boldsymbol{u}(t), t)d\tau + J(\mathbf{x} + \Delta\mathbf{x}, t + \Delta t) \end{aligned} \tag{24}$$

where τ is a dummy variable. We note that the cost-to-go function in Eq. (24) is updated recursively, where $\boldsymbol{x}+\Delta\boldsymbol{x}$ is the state at time $t+\Delta t$ which is computed as a system response for $\boldsymbol{x}(t)$ and $\boldsymbol{u}(t)$. Among all the potential costs to go from time t to tf, given by Eq. (24), we select only the candidates $J*(\boldsymbol{x}(t), t)$ that optimize the function $J(\boldsymbol{x}(t), t)$ within the interval $[t+\Delta t, tf]$. Assuming that the optimal

cost $J^*(\boldsymbol{x}+\Delta\boldsymbol{x}, t+\Delta t)$ and control law $\boldsymbol{u}(t+\Delta t)$ are known for all $\boldsymbol{x}+\Delta\boldsymbol{x}$, we can therefore compute optimal control law $\boldsymbol{u}(t)$ for all $\boldsymbol{x}(t)$ on the time interval $[t, t+\Delta t]$ through the corresponding minimization procedure

$$J^*(\mathbf{x}(t),t) = \min_{\mathbf{u}(T)\in\mathbb{R}^n}\left\{\int_t^{t+\Delta t} L(\mathbf{x}(t),\boldsymbol{u}(t),t)d\tau + J^*(\mathbf{x}(t+\Delta t),t+\Delta t)\right\} \tag{25}$$

which casts the principle of optimality on $\tau\in[t, t+\Delta t]$. By finding the Taylor series expansion of the right hand side of Eq. (25) around the point $(\boldsymbol{x}(t), t)$, we get

$$\min_{\mathbf{u}(T)\in\mathbb{R}^n}\left\{L(\mathbf{x}(t),\boldsymbol{u}(t),t)\Delta t + J^*(\mathbf{x}(t),t) + \frac{\partial J^*(\mathbf{x}(t),t)}{\partial t}\Delta t + \frac{\partial J^*(\mathbf{x}(t),t)}{\partial \mathbf{x}}\dot{\mathbf{x}}(t)\Delta t\right\} \tag{26}$$

Through a minor manipulation of Eq. (27) and by taking the limit as $\Delta t \to 0$, we can derive the partial differential equation that governs the optimal cost $J^*(\boldsymbol{x}(t), t)$

$$-\frac{\partial J^*(\mathbf{x}(t),t)}{\partial t} = \min_{\mathbf{u}(T)\in\mathbb{R}^n}\left\{L(\mathbf{x}(t),\boldsymbol{u}(t),t) + \left(\frac{\partial J^*(\mathbf{x}(t),t)}{\partial x}\right)^T\cdot\dot{\mathbf{x}}(t)\right\} \tag{27}$$

where the result is denoted as the Hamilton-Jacobi-Bellman (HJB) equation. If we denote the Lagrange multipliers as $\partial J^*(\boldsymbol{x}(t), t)\partial\boldsymbol{x} = \boldsymbol{\lambda}(t)$, and the state equation as $\dot{\boldsymbol{x}}(t) = \boldsymbol{f}\big(\boldsymbol{x}(t),\boldsymbol{u}(t)\big)$, we can rewrite the HJB equation as follows

$$-\frac{\partial J^*(\mathbf{x}(t),t)}{\partial t} = \min_{\mathbf{u}(T)\in\mathbb{R}^n}\{L(\mathbf{x}(t),\boldsymbol{u}(t),t) + \boldsymbol{\lambda}^T(t)\cdot\mathbf{f}(\mathbf{x}(t),\boldsymbol{u}(t),t)\} \tag{28}$$

The result in Eq. (28) can be recast in a more standard form that employs the Hamiltonian $H(\boldsymbol{x}(t), \boldsymbol{u}(t), \boldsymbol{\lambda}(t), t)$ in place of the Lagrangian $L(\boldsymbol{x}(t), \boldsymbol{u}(t), t)$, where the relation is given as

$$H(\mathbf{x}(t),\mathbf{u}(t),\boldsymbol{\lambda}(t),t) = L(\mathbf{x}(t),\mathbf{u}(t),t) + \boldsymbol{\lambda}^T(t)\cdot\mathbf{f}(\mathbf{x}(t),\mathbf{u}(t),t) \tag{29}$$

We can further introduce the result Eq. (29) into the HJB equation in Eq. (28), which results

$$-\frac{\partial J^*(\mathbf{x}(t),t)}{\partial t} = \min_{\mathbf{u}(T)\in\mathbb{R}^n}\{H(\mathbf{x}(t),\mathbf{u}(t),\boldsymbol{\lambda}(t),t)\} \tag{30}$$

The result obtained in Eq. (30) yields the optimal control law for a nonlinear system using closed-loop or state feedback, where the solution, in most cases, can only be obtained numerically.

3.3 Mixed linear quadratic regulator (LQR) algorithm

Here we present the advanced control algorithm, denoted as linear quadratic regulator (LQR), which optimizes both the control effort (minimal control energy). In order to determine the optimal control law $\mathbf{u}^*(t)$, we first define the cost-to-go function $J(\boldsymbol{x}(t), t)$ as a quadratic form

$$J(\mathbf{x}(t),t) = \frac{1}{2}\mathbf{x}^T(t_f)\cdot\mathbf{Q}_f\mathbf{x}(t_f) + \frac{1}{2}\int_{t_0}^{t_f}\big(\mathbf{x}(t)\cdot\mathbf{Q}\mathbf{x}(t) + \boldsymbol{u}(t)\cdot\mathbf{R}\mathbf{u}(t)\big)dt \tag{31}$$

where $\boldsymbol{Q} = \boldsymbol{Q}T > 0$, $\boldsymbol{Q}f$ and $\boldsymbol{R} = \boldsymbol{R}T>0$ are matrices related to the penalty of state error, terminalerror and control effort. According to Eq. (29) we can define the Hamiltonian as follows

$$H(\mathbf{x}(t),\boldsymbol{u}(t),\boldsymbol{\lambda}(t),t) = \frac{1}{2}\big(\mathbf{x}^T(t)\cdot\mathbf{Q}\mathbf{x}(t) + \mathbf{u}^T(t)\mathbf{R}\cdot\mathbf{u}(t)\big) + \boldsymbol{\lambda}^T(t)\cdot\big(\mathbf{A}(t)\mathbf{x}(t) + \mathbf{B}\mathbf{u}(t)\big) \tag{32}$$

To perform optimization of function in Eq. (31), we employ the HJB principle in Eq. (30), where the minimization task reads

$$-\frac{\partial J^*}{\partial t} = \min_{\mathbf{u}(T)\in\mathbb{R}^n}\left\{\frac{1}{2}(\mathbf{x}^T\cdot\mathbf{Q}\mathbf{x} + \mathbf{u}^T\mathbf{R}\cdot\mathbf{u}) + \boldsymbol{\lambda}^T\cdot(\mathbf{A}\mathbf{x} + \mathbf{B}\mathbf{u})\right\} \tag{33}$$

Now, we can obtain stationary condition, state and co-state equations by finding the first derivative of the H with respect to $\boldsymbol{u}$, $\boldsymbol{x}$ and $\boldsymbol{\lambda}$, respectively.

$$-\dot{\boldsymbol{\lambda}} = \left(\frac{\partial H}{\partial \mathrm{x}}\right) = \mathbf{Q}\mathbf{x} + \mathbf{A}^T\boldsymbol{\lambda}$$
$$\dot{\mathbf{x}} = \left(\frac{\partial H}{\partial \boldsymbol{\lambda}}\right) = \mathbf{A}\mathbf{x} + \mathbf{B}\mathbf{u}^* \tag{34}$$

where we obtain the optimal control law $\boldsymbol{u}^*(\boldsymbol{\lambda}(t),t)$ which minimizes the functional in Eq. (33). The result in Eq. (34) can be rewritten in matrix form as

$$\begin{Bmatrix}\dot{\mathbf{x}}\\ \dot{\boldsymbol{\lambda}}\end{Bmatrix} = \begin{bmatrix}\mathbf{A} & -\mathbf{B}\mathbf{R}^{-1}\mathbf{B}^T\\ -\mathbf{Q} & -\mathbf{A}^T\end{bmatrix}\begin{Bmatrix}\mathbf{x}\\ \boldsymbol{\lambda}\end{Bmatrix} \tag{35}$$

To provide the closed-loop or state feedback control, we redefine $\mathbf{u}^*(\boldsymbol{\lambda}(t), t)$ in terms of $\boldsymbol{x}(t)$. If we assume that the optimal cost-to-go function has a following solution form $J^*(\boldsymbol{x}(t), t) = 12\boldsymbol{x}T\cdot\boldsymbol{S}(t)\boldsymbol{x}$, where $\boldsymbol{S}(t) = \boldsymbol{S}T(t) > 0$, then the Lagrange multipliers and time variation of the cost-to-go function can be given as

$$\frac{\partial J^*}{\partial \mathbf{x}} = \mathbf{S}(t)\mathbf{x} \equiv \boldsymbol{\lambda}; \quad \frac{\partial J^*}{\partial t} = \frac{1}{2}\mathbf{x}^T\cdot\dot{\mathbf{S}}(t)\mathbf{x}; \tag{36}$$

Now, we can rewrite the optimal control law $\mathbf{u}^*(\boldsymbol{x}, t)$

in Eq. (34) as

$$\mathbf{u}^*(\mathbf{x},t) = \mathbf{R}^{-1}\mathbf{B}^T\mathbf{S}(t)\mathbf{x} \quad (37)$$

where $-\boldsymbol{R}{-}1\boldsymbol{BTS}(t)$ is denoted as Kalman gain. By combining the results in Eqs. (35), (36) and (37), one can cast the Riccati differential equation in matrix form as follows

$$-\dot{\mathbf{S}}(t) = \mathbf{Q} - \mathbf{S}(t)\mathbf{B}\mathbf{R}^{-1}\mathbf{B}^T\mathbf{S}(t) + \mathbf{S}(t)\mathbf{A} + \mathbf{A}^T\mathbf{S}(t) \quad (38)$$

where the final state condition is given $\boldsymbol{S}(tf) = \boldsymbol{Q}f$. For clarification, the solution procedure of the LQR problem reduces to numerical integration of the Riccati differential equation Eq. (38) backwards in time. Once the solution $\boldsymbol{S}(t)$ is obtained, we can compute the optimal feedback gain $\mathbf{u}^*(t)$ at the time t (see Eq. (37)), and then update the state equation

$$\dot{\mathbf{x}}(t) = \big(\mathbf{A}(t) - \mathbf{B}\mathbf{R}^{-1}\mathbf{B}^T\mathbf{S}(t)\big)\mathbf{x}(t) \quad (39)$$

Thus, we can proceed with the computation of the system response forward in time for the given control signal in Eq. (37).

4. Numerical examples

The most important concept in control system analysis and design tools is stability. Stability analysis of fuzzy control systems has always been difficult because fuzzy systems are essentially nonlinear systems. Recently, some useful stability techniques based on nonlinear stability theory (Wang *et al*. 2024e) have been was raised. One of the authors derived stability conditions and robust stability conditions from the definition of stability in the Lyapunov sense. Therefore, when analyzing fuzzy control systems, we need at least a fuzzy model of the system. In this paper, it is assumed that the fuzzy model of the target system has been identified. Therefore, the well-known TS fuzzy model is adopted. The details of the TS fuzzy model are described below.

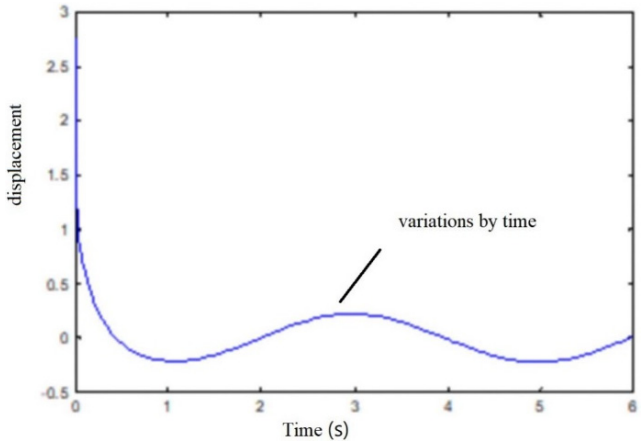

Fig. 4 Limit cycle of the test nonlinear structural system

Plant Rule 1:

If $x_1(t)$ is $M_{i\,1}$ and $\cdots$ and $x_g(t)$ is $M_{\rightleftarrows i\rightleftarrows g\rightleftarrows}$
then $\dot{x}(t) = A_{i\rightleftarrows}x(t) + B_{i\rightleftarrows}u(t)$; $i = 1, 2, \cdots, r$

In this example, we first verify the unit control algorithm in the case where both the stiffness and mass matrices are constant over time. We perform numerical calculations using Euler's backward time integration scheme. To avoid amplitude decay (also called numerical damping) due to insufficient accuracy of the scheme, we use a very small time step Δ falcon = 0.0001 s, where 1 s has a step size of 10^4. First, we verified the accuracy of the proposed free vibration unit without controlling the system's response to the initial state of the state space model in Matlab, by calling the functions (sys = ss(A, B, C, D)] and [[y, t] = initial value (sys,x0)). Consider the fuzzy system through the TS fuzzy continuous model, described as follows.

Rule 1: If $x_1(t)$ is M_{11}
Then $\dot{x}(t) = A_1x(t)$ with $A_1 = \begin{bmatrix} -29 & 1 \\ 3 & -12 \end{bmatrix}$
Rule 2: If $x_1(t)$ is M_{21}
Then $\dot{x}(t) = A_2x(t)$, with $A_2 = \begin{bmatrix} -25 & -4 \\ 5 & -14 \end{bmatrix}$

and membership functions for Rule 1 and Rule 2 are

$$M_{11}\big(x_1(t)\big) = \frac{1}{1+exp[-\,2x_1(t)]},$$
$$M_{21}\big(x_1(t)\big) = 1 - M_{11}\big(x_1(t)\big).$$

In order to satisfy the stability conditions, hence, we can obtain the following matrix $P = \begin{bmatrix} 1.5062 & -0.2794 \\ -0.2794 & 1.7619 \end{bmatrix}$ by using LMI optimization algorithms with the limit cycle shown in Fig. 4. The algebraic Riccati equation lqr ([K,S,P] = lqr(A,B,Q,R,N)) and the differential algebraic Riccati equation idare ([X,L,G] = idare(A,B,Q) Algorithm, R)). These algorithms provide steady-state and time-discrete solutions to the differential Riccati equations. Calculated with different penalty state error values: $\boldsymbol{Q} = q\boldsymbol{I}$, q = (0, 10, 10^2, 10^3, 10^4) and $\boldsymbol{R} = r\boldsymbol{I}$, r =1. Nonlinear effects can affect problems in a variety of ways. A classic example is a nonlinear spring, where the restoring force is not linearly proportional to the displacement. For the case of symmetric nonlinearity (compression or stretching has the same effect), the equation of motion is the system undamped and there are periodic solutions where the natural frequency increases with amplitude. This model is often called the Duffin equation, named after the mathematician who studied it.

If a system is acted upon by a periodic force, in classical theory we assume that the output will also be periodic. But nonlinear vibration theory relies on the assumption that periodic inputs produce periodic outputs. However, it is this assumption that is challenged in the new theory of chaotic vibrations. The oscillation amplitude of the displacement decreases from the initial value of 1 to zero at a time slightly larger than 0.2 s. The speed changes from an initial value of zero to a value around -7 and drops to zero at 0.3

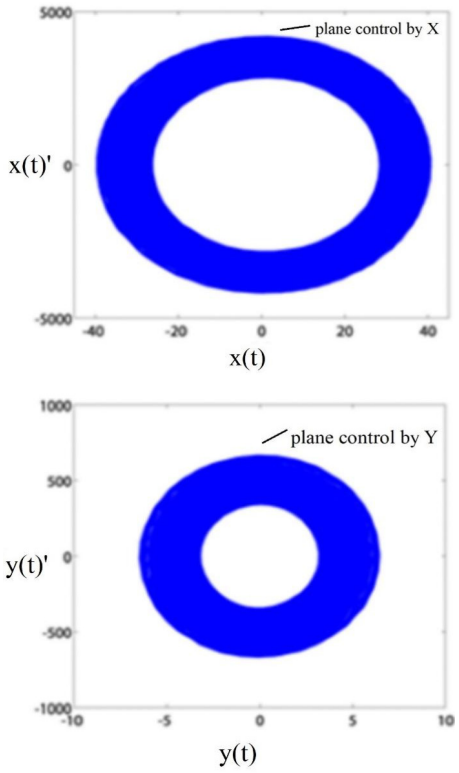

Fig. 5 Phase plane control of fuzzy calculations

seconds. When the control law is equal to 0 when q = 0, as the penalty value q increases, the control law exhibits oscillation characteristics, and the oscillation amplitude increases with the increase of q. When q = 10^4, the oscillation characteristic of the control signal disappears.

The same seismic excitation was selected as in reference of Chen *et al*. (2023a, b) for testing, and a 6-story shear type building model was utilized as the experimental object. Each floor had a height of 3.4 m and a stiffness value of 12000 KN/m. It shows the peak control force results of concrete structures under seismic excitation. In the control of multi-layer structures, MRFD and FC were installed in each floor to ensure the control effect of lateral displacement of the floors. There were significant differences in the SC effects among the three types of SCs in multi-floor SC. In FC, MRFDs were installed on each floor to reduce lateral forces. In the comparison of lateral displacement, the total lateral displacement without control was 90 cm, LQR control was 45 cm, and FC was 49 cm. Overall, FC dynamically adjusted lateral effects and had the best stability among the three. At the same time, in the comparison of acceleration peaks, the total acceleration peak of FC was 37 m/s^2, and the LQR control was 34 m/s^2. Due to the placement of MRFDs in different floors of FC, the building acceleration was effectively controlled. FC had better control effects. At the same time, in actual building SC, it was also necessary to consider the impact of output variables on SC, including open-loop control with seismic acceleration as input, closed-loop control with floor acceleration and displacement as input, and closed-loop open control with seismic acceleration and displacement as input. Phase plane control of fuzzy calculations is as Fig. 5 and the control results under different inputs under FC are shown in Fig. 6.

5. Conclusions

We have explored the efficiency of the time varying advanced control algorithm applied to nonlinear structural dynamic model. We chose the linear-quadratic regulator (LQR) algorithm to drive the system into the desired state, where the optimal control strategy considers minimization task of the cost-to-go functional with respect to the state error and control effort. Due to the nonlinear nature of kinematics, the proposed optimization task reduces to the computation of the differential Riccati's equation in each time step. In addition, in comprehensive comparison, the proposed FC technology did not damage the concrete structure, while the other two methods both had certain structural damage. The proposed technology had better application effects and met the SC requirements of actual earthquake scenarios in buildings. In the research, fuzzy DC strategy is mainly used and compared with traditional linear quadratic regulator (LQR) control strategy. LQR can obtain the optimal control law with linear feedback of the state, which is easy to form closed-loop optimal control. LQR optimal control can achieve good performance indicators of the original system at low cost. Therefore, fuzzy DC is adopted between floors, and LQR centralized control concept is adopted throughout the entire building control.

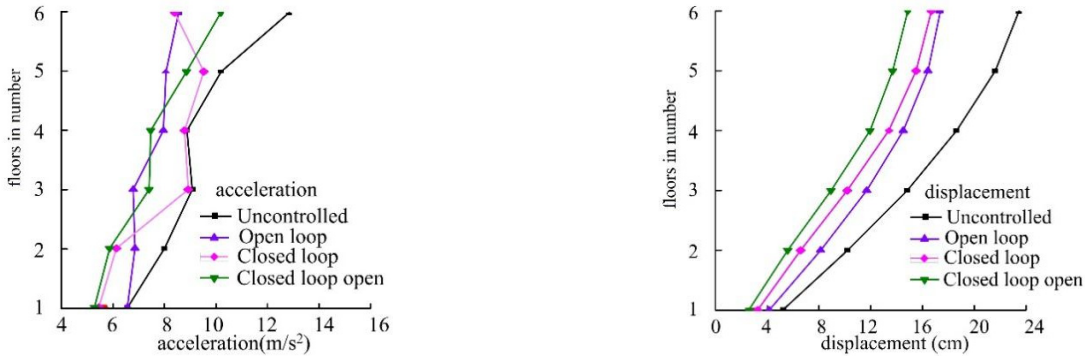

Fig. 6 Peak acceleration and displacement results under different control inputs

Data availability

The datasets used and/or analysed during the current study available from the corresponding author on reasonable request.

References

Ahmad, I. and Shokouhian, M. (2024), "Promoting Sustainable Green Infrastructure: Experimental and Numerical Investigation of Concrete Reinforced with Recycled Steel Fibers", *Arch. Adv. Eng. Sci.* https://doi.org/10.47852/bonviewAAES42022837

Ariyanto, M., Refat, C.M.M., Hirao, K. and Morishima, K. (2023), "Movement optimization for a cyborg cockroach in a bounded space incorporating machine learning", *Cyborg Bionic Syst.*, **4**. https://doi.org/10.34133/cbsystems.0012

Cai, Z., Zhang, T., Jing, X.Y. and Shao, L. (2022), "Unequal adaptive visual recognition by learning from multi-modal data", *Inform. Sci.*, **600**, 1-21. https://doi.org/10.1016/j.ins.2022.03.076

Cai, Z., Zhang, T., Ma, F. and Jing, X.Y. (2022), "Dual contrastive universal adaptation network for multi-source visual recognition", *Knowledge-Based Syst.*, **254**, p. 109632. https://doi.org/10.1016/j.knosys.2022.109632

Cao, J., Du, J., Zhang, H., He, H., Bao, C. and Liu, Y. (2024), "Mechanical properties of multi-bolted Glulam connection with slotted-in steel plates", *Constr. Build. Mater.*, **433**, p. 136608. https://doi.org/10.1016/j.conbuildmat.2024.136608

Casciati, S., Chassiakos, A.G. and Masri, S.F. (2014), "Toward a paradigm for civil structural control", *Smart Struct. Syst., Int. J.*, **14**(5), 981-1004. https://doi.org/10.12989/sss.2014.14.5.981

Chai, S., Wang, S., Liu, C., Liu, X., Liu, T. and Yang, R. (2024), "A visual measurement algorithm for vibration displacement of rotating body using semantic segmentation network", *Expert Syst. Applicat.*, **237**, p. 121306. https://doi.org/10.1016/j.eswa.2023.121306

Chen, Y. (2022), "Research on collaborative innovation of key common technologies in new energy vehicle industry based on digital twin technology", *Energy Reports*, **8**, 15399-15407. https://doi.org/10.1016/j.egyr.2022.11.120

Chen, C.W. (2023), "A criterion of robustness intelligent nonlinear control for multiple time-delay systems based on fuzzy Lyapunov methods", *Nonlin. Dyn.*, **76**, 23-31. https://doi.org/10.1007/s11071-013-0869-9

Chen, H., Jing, X.Y., Li, Z., Wu, D., Peng, Y. and Huang, Z. (2020), "An empirical study on heterogeneous defect prediction approaches", *IEEE Transact. Softw. Eng.*, **47**(12), 2803-2822. https://doi.org/10.1109/TSE.2020.2968520

Chen, B., Hu, J., Zhao, Y. and Ghosh, B.K. (2022a), "Finite-time observer based tracking control of uncertain heterogeneous underwater vehicles using adaptive sliding mode approach", *Neurocomputing*, **481**, 322-332. https://doi.org/10.1016/j.neucom.2022.01.038

Chen, H., Jing, X.Y., Zhou, Y., Li, B. and Xu, B. (2022b), "Aligned metric representation based balanced multiset ensemble learning for heterogeneous defect prediction", *Inform. Softw. Technol.*, **147**, p. 106892. https://doi.org/10.1016/j.infsof.2022.106892

Chen, R., Jing, X.Y., Wu, F., Zheng, W. and Hao, Y. (2023a), "Taskspecific parameter decoupling for class incremental learning", *Inform. Sci.*, **651**, p. 119731. https://doi.org/10.1016/j.ins.2023.119731

Chen, Z.Y., Wang, R.Y., Meng, Y. and Chen, T. (2023b), "A novel grey TMD control for structures subjected to earthquakes", *Earthq. Struct., Int. J.*, **24**(1), 1-9. https://doi.org/10.12989/eas.2023.24.1.001

Cheng, L., Jing, X.Y., Zhu, X., Hu, C.H., Gao, G. and Wu, S. (2020), "Local and global aligned spatiotemporal attention network for video-based person re-identification", *Multimedia Tools Appl.*, **79**, 34489-34512. https://doi.org/10.1007/s11042-020-08765-1

Du, G., Zhang, H., Yu, H., Hou, P., He, J., Cao, S., Wang, G. and Ma, L. (2024), "Study on automatic tracking system of microwave deicing device for railway contact wire", *IEEE Transact. Instrument. Measur.*, **73**, 1-11. https://doi.org/10.1109/TIM.2024.3446638

Fu, Q., Luo, K., Song, Y., Zhang, M., Zhang, S., Zhan, J. and Li, Y. (2022), "Study of sea fog environment polarization transmission characteristics", *Appl. Sci.*, **12**(17), p. 8892. https://doi.org/10.3390/app12178892

Guo, C., Hu, J., Hao, J., Čelikovský, S. and Hu, X. (2023), "Fixed-time safe tracking control of uncertain high-order nonlinear pure-feedback systems via unified transformation functions", *Kybernetika*, **59**(3), 342-364. https://doi.org/10.14736/kyb-2023-3-0342

Hao, Y., Jing, X.Y. and Sun, Q. (2022), "Joint learning sample similarity and correlation representation for cancer survival prediction", *BMC Bioinform.*, **23**(1), p. 553. https://doi.org/10.1186/s12859-022-05110-1

Hirao, Y., Wan, W., Kanoulas, D. and Harada, K. (2023), "Body extension by using two Mobile manipulators", *Cyborg Bionic Syst.*, **4**, p. 0014. https://doi.org/10.34133/cbsystems.0014

Kai, Y. and Yin, Z. (2022), "Linear structure and soliton molecules of Sharma-Tasso-Olver-Burgers equation", *Phys. Lett. A*, **452**, p. 128430. https://doi.org/10.1016/j.physleta.2022.128430

Li, M., Wang, T., Chu, F., Han, Q., Qin, Z. and Zuo, M.J. (2021), "Scaling-basis chirplet transform", *IEEE Transact. Indust. Electron.*, **68**(9), 8777-8788. https://doi.org/10.1109/TIE.2020.3013537

Li, H., Lu, H. and Li, Q. (2024a), "Numerical investigations of the influences of valve spool structure on the eccentric jet flow characteristic in high-pressure angle valves", *Energy*, **298**, p. 131378. https://doi.org/10.1016/j.energy.2024.131378

Li, X., Liu, Y., Ge, L. and Zhang, Z. (2024b), "A large-stroke reluctance-actuated nanopositioner: Compliant compensator for enhanced linearity and precision motion control", *IEEE/ASME Transact. Mechatron.*, **29**(4), 2947-2955. https://doi.org/10.1109/TMECH.2024.3405195

Liu, Y., Jiang, D., Yun, J., Sun, Y., Li, C., Jiang, G., Kong, J., Tao, B. and Fang, Z. (2022), "Self-tuning control of manipulator positioning based on fuzzy PID and PSO algorithm", *Front. Bioeng. Biotechnol.*, **9**, p. 817723. https://doi.org/10.3389/fbioe.2021.817723

Liu, L., Zhang, S., Zhang, L., Pan, G. and Yu, J. (2023), "Multi-UUV Maneuvering Counter-Game for Dynamic Target Scenario Based on Fractional-Order Recurrent Neural Network", *IEEE Transact. Cybernet.*, **53**(6), 4015-4028. https://doi.org/10.1109/TCYB.2022.3225106

Ma, K., Li, Z., Liu, P., Yang, J., Geng, Y., Yang, B. and Guan, X. (2021), "Reliability-constrained throughput optimization of industrial wireless sensor networks with energy harvesting relay", *IEEE Internet Things J.*, **8**(17), 13343-13354. https://doi.org/1109/jiot.2021.3065966

Meng, Q., Ma, Q. and Shi, Y. (2023), "Adaptive fixed-time stabilization for a class of uncertain nonlinear systems", *IEEE Transact. Automat. Control*, **68**(11), 6929-6936. https://doi.org/10.1109/TAC.2023.3244151

Miaofen, L., Youmin, L., Tianyang, W., Fulei, C. and Zhike, P. (2023), "Adaptive synchronous demodulation transform with application to analyzing multicomponent signals for machinery fault diagnostics", *Mech. Syst. Signal Process.*, **191**, p. 110208. https://doi.org/10.1016/j.ymssp.2023.110208

Mohammadzadeh, A., Taghavifar, H., Zhang, C., Alattas, K.A., Liu, J. and Vu, M.T. (2024), "A non-linear fractional-order type-3 fuzzy control for enhanced path-tracking performance of autonomous cars", *IET Control Theory Applicat*., **18**(1), 40-54. https://doi.org/10.1049/cth2.12538

Niu, J., Li, Z., Chen, H., Dong, X. and Jing, X.Y. (2022), "Data sampling and kernel manifold discriminant alignment for mixed-project heterogeneous defect prediction", *Softw. Quality J*., **30**(4), 917-951. https://doi.org/10.1007/s11219-022-09588-z/

Qu, J., Mao, B., Li, Z., Xu, Y., Zhou, K., Cao, X. and Wang, X. (2023), "Recent progress in advanced tactile sensing technologies for soft grippers", *Adv. Funct. Mater*., **33**(41), p. 2306249. https://doi.org/10.1002/adfm.202306249

Sakthivel, R., Anusuya, S., Kwon, O.M. and Mohanapriya, S. (2023), "Composite fault reconstruction and fault-tolerant control design for cyber-physical systems: An interval type-2 fuzzy approach", *ISA Transactions*, **143**, 38-49. https://doi.org/10.1016/j.isatra.2023.10.002

Samimy, M., Webb, N., Esfahani, A. and Leahy, R. (2023), "Perturbation-based active flow control in over expanded to under expanded supersonic rectangular twin jets", *J. Fluid Mech*., **959**, p. A13. https://doi.org/10.1017/jfm.2023.139

She, A., Wang, L., Peng, Y. and Li, J. (2023), "Structural reliability analysis based on improved wolf pack algorithm AK-SS", *Structures*, **57**, p. 105289. https://doi.org/10.1016/j.istruc.2023.105289

Shi, M., Lv, L. and Xu, L. (2023a), "A multi-fidelity surrogate model based on extreme support vector regression: fusing different fidelity data for engineering design", *Eng. Computat*., **40**(2), 473-493. https://doi.org/10.1108/EC-10-2021-0583

Shi, Y., Hou, X., Na, Z., Zhou, J., Yu, N., Liu, S., Xin, L., Gao, G. and Liu, Y. (2023b), "Bio-inspired attachment mechanism of dynastes Hercules: Vertical climbing for on-orbit assembly legged robots", *J. Bionic Eng*., **21**(1), 137-148. https://doi.org/10.1007/s42235-023-00423-0

Shu, J., Yu, H., Liu, G., Duan, Y., Hu, H. and Zhang, H. (2025), "DF-CDM: Conditional diffusion model with data fusion for structural dynamic response reconstruction", *Mech. Syst. Signal Process*., **222**, p. 111783. https://doi.org/10.1016/j.ymssp.2024.111783

Song, F., Liu, Y., Dong, Y., Chen, X. and Tan, J. (2024), "Motion Control of Wafer Scanners in Lithography Systems: From Setpoint Generation to Multi-Stage Coordination", *IEEE Transact. Instrument. Measure*. https://doi.org/10.1109/TIM.2024.3413202

Tan, J., Zhang, K., Li, B. and Wu, A.G. (2023), "Event-triggered sliding mode control for spacecraft reorientation with multiple attitude constraints", *IEEE Transact. Aerosp. Electron. Syst.*, **59**(5), 6031-6043. https://doi.org/10.1109/TAES.2023.3270391

Tian, H., Zhao, M., Liu, J., Wang, Q., Yu, X. and Wang, Z. (2024a), "Dynamic Analysis and Sliding Mode Synchronization Control of Chaotic Systems with Conditional Symmetric Fractional-Order Memristors", *Fractal Fractional*, **8**(6), p. 307. https://doi.org/10.3390/fractalfract8060307

Tian, G., Tan, J., Li, B. and Duan, G. (2024b), "Optimal fully actuated system approach-based trajectory tracking control for robot manipulators", *IEEE Transact. Cybernet.*, **54**(12), 7469-7478. https://doi.org/10.1109/TCYB.2024.3467386

Toma, S. and Chen, W.F. (2024), "A Study on Safety Criteria for Toppling of Pile Drivers and Cranes Based on Structural Stability", *Arch. Adv. Eng. Sci*. https://doi.org/10.47852/bonviewAAES42022138

Wang, Y. and Sigmund, O. (2023), "Multi-material topology optimization for maximizing structural stability under thermo-mechanical loading", *Comput. Methods Appl. Mech. Eng*., **407**, p. 115938. https://doi.org/10.1016/j.cma.2023.115938

Wang, Y. and Sigmund, O. (2024), "Topology optimization of multi-material active structures to reduce energy consumption and carbon footprint", *Struct. Multidiscipl. Optimiz*., **67**(1), p. 5. https://doi.org/10.1007/s00158-023-03698-3

Wang, Y., Chen, H., Law, J., Du, X. and Yu, J. (2023a), "Ultrafast miniature robotic swimmers with upstream motility", *Cyborg Bionic Syst*., **4**. https://doi.org/10.34133/cbsystems.0015

Wang, K., Boonpratatong, A., Chen, W., Ren, L., Wei, G., Qian, Z., Lu, X. and Zhao, D. (2023b), "The fundamental property of human leg during walking: linearity and nonlinearity", *IEEE Transact. Neural Syst. Rehabilit. Eng.*, **31**, 4871-4881. https://doi.org/10.1109/TNSRE.2023.3339801

Wang, J., Li, Y., Wu, Y., Liu, Z., Chen, K. and Chen, C.P. (2024a), "Fixed-time formation control for uncertain nonlinear multi-agent systems with time-varying actuator failures", *IEEE Transact. Fuzzy Syst*., **32**(4), 1965-1977. https://doi.org/10.1109/TFUZZ.2023.3342282

Wang, J., Wu, Y., Chen, C.L.P., Liu, Z. and Wu, W. (2024b), "Adaptive PI event-triggered control for MIMO nonlinear systems with input delay", *Inform. Sci*., **677**, p. 120817. https://doi.org/10.1016/j.ins.2024.120817

Wang, S., Lin, S. and Yang, R. (2024c), "A lightweight convolutional neural network for multipoint displacement measurements on bridge structures", *Nonlinear Dyn*., **112**(14), 11745-11763. https://doi.org/10.1007/s11071-024-09673-x

Wang, X., Zhang, R., Miao, Y., Wang, S. and Zhang, Y. (2024d), "PI^2-Based Adaptive Impedance Control for Gait Adaption of Lower Limb Exoskeleton", *IEEE/ASME Transact. Mechatron*. https://doi.org/10.1109/TMECH.2024.3370954

Wang, M., Kang, J., Liu, W., Li, M., Su, J., Fang, Z., Li, X., Shang, L., Zhang, F. and Guo, C. (2024e), "Design and study of mine silo drainage method based on fuzzy control and Avoiding Peak Filling Valley strategy", *Scientific Reports*, **14**(1), 9300. https://doi.org/10.1038/s41598-024-60228-x

Wu, J., Wang, Y. and Yin, C. (2022), "Curvilinear Multilane Merging and Platooning With Bounded Control in Curved Road Coordinates", *IEEE Transact. Vehicul. Technol*., **71**(2), 1237-1252. https://doi.org/10.1109/TVT.2021.3131751

Xu, X. and Li, B. (2024), "PDE-based observation and predictor-based control for linear systems with distributed infinite input and output delays", *Automatica*, **170**, p. 111845. https://doi.org/10.1016/j.automatica.2024.111845

Xu, B., Wang, X., Zhang, J., Guo, Y. and Razzaqi, A.A. (2022), "A novel adaptive filtering for cooperative localization under compass failure and non-gaussian noise", *IEEE Transact. Vehicul. Technol.*, **71**(4), 3737-3749. https://doi.org/10.1109/TVT.2022.3145095

Yin, Y., Wang, Z., Zheng, L., Su, Q. and Guo, Y. (2024), "Autonomous UAV Navigation with Adaptive Control Based on Deep Reinforcement Learning", *Electronics*, **13**(13), p. 2432. https://doi.org/10.3390/electronics13132432

Zhang, X., Li, S., Jing, X.Y., Ma, F. and Zhu, C. (2020), "Unsupervised domain adaption for image-to-video person reidentification", *Multimedia Tools Appl*., **79**, 33793-33810. https://doi.org/10.1007/s11042-019-08550-9

Zhang, X., Liu, Y., Chen, X., Li, Z. and Su, C.Y. (2023), "Adaptive pseudoinverse control for constrained hysteretic nonlinear systems and its application on dielectric elastomer actuator", *IEEE/ASME Transact. Mechatron*., **28**(4), 2142-2154. https://doi.org/10.1109/TMECH.2022.3231263

Zhang, L., Ma, C. and Liu, J. (2024), "Enhancing four-axis machining center accuracy through interactive fusion of spatiotemporal graph convolutional networks and an error-controlled digital twin system", *J. Manuf. Processes*, **112**, 14-31. https://doi.org/10.1016/j.jmapro.2024.01.024

Zheng, C., An, Y., Wang, Z., Wu, H., Qin, X., Eynard, B. and Zhang, Y. (2022), "Hybrid offline programming method for robotic welding systems", *Robot. Comput.-Integr. Manuf*., **73**,

p. 102238. https://doi.org/10.1016/j.rcim.2021.102238
Zheng, C., An, Y., Wang, Z., Qin, X., Eynard, B., Bricogne, M., Le Duigou, J. and Zhang, Y. (2023), "Knowledge-based engineering approach for defining robotic manufacturing system architectures", *Int. J. Product. Res.*, **61**(5), 1436-1454. https://doi.org/10.1080/00207543.2022.2037025
Zhou, C. (2023), "Development Expectation Gap of Design-Build Contract Delivery in China's Civil Aviation Infrastructure Projects", *Arch. Adv. Eng. Sci.* https://doi.org/10.47852/bonviewAAES32021430
Zhou, Z., Wang, Y., Zhou, G., Nam, K., Ji, Z. and Yin, C. (2023), "A twisted Gaussian risk model considering target vehicle longitudinal-lateral motion states for host vehicle trajectory planning", *IEEE Transact. Intell. Transport. Syst.*, **24**(12), 13685-13697. https://doi.org/10.1109/TITS.2023.3298110
Zhou, Y., Song, Y., Zhao, S., Li, X., Shao, L., Yan, H., Xu, Z. and Ding, S. (2024), "A comprehensive aerodynamic-thermal-mechanical design method for fast response turbocharger applied in aviation piston engines", *Propuls. Power Res.*, **13**(2), 145-165. https://doi.org/10.1016/j.jppr.2024.04.001
Zhu, C., Li, X., Leung, V.C., Yang, L.T., Ngai, E.C.H. and Shu, L. (2017), "Towards pricing for sensor-cloud", *IEEE Transact. Cloud Comput.*, **8**(4), 1018-1029. https://doi.org/10.1109/TCC.2017.2649525
Zhu, C. (2023), "Intelligent robot path planning and navigation based on reinforcement learning and adaptive control", *J. Logist. Inform. Service Sci.*, **10**(3), 235-248. https://doi.org/10.33168/JLISS.2023.0318